Heme binding by *Corynebacterium diphtheriae* HmuT: Function and heme environment

Supporting Information

Elizabeth B. Draganova,[†] Neval Akbas,[†] Seth A. Adrian,[§] Gudrun S. Lukat-Rodgers,[§] Daniel P. Collins,[‡] John H. Dawson, [‡] Courtni E. Allen,[Δ] Michael P. Schmitt, [Δ] Kenton R. Rodgers,[§,] and Dabney W. Dixon[†,*]*

[†]Department of Chemistry, Georgia State University, Atlanta, Georgia 30302-3965
[§]Department of Chemistry and Biochemistry, North Dakota State University, Fargo, North Dakota 58108-6050
[‡]Department of Chemistry and Biochemistry, University of South Carolina, Columbia, South Carolina 29208
[Δ]Laboratory of Respiratory and Special Pathogens, Division of Bacterial, Parasitic, and Allergenic Products, Center for Biologics Evaluation, and Research, Food and Drug Administration, Silver Spring, Maryland 20993

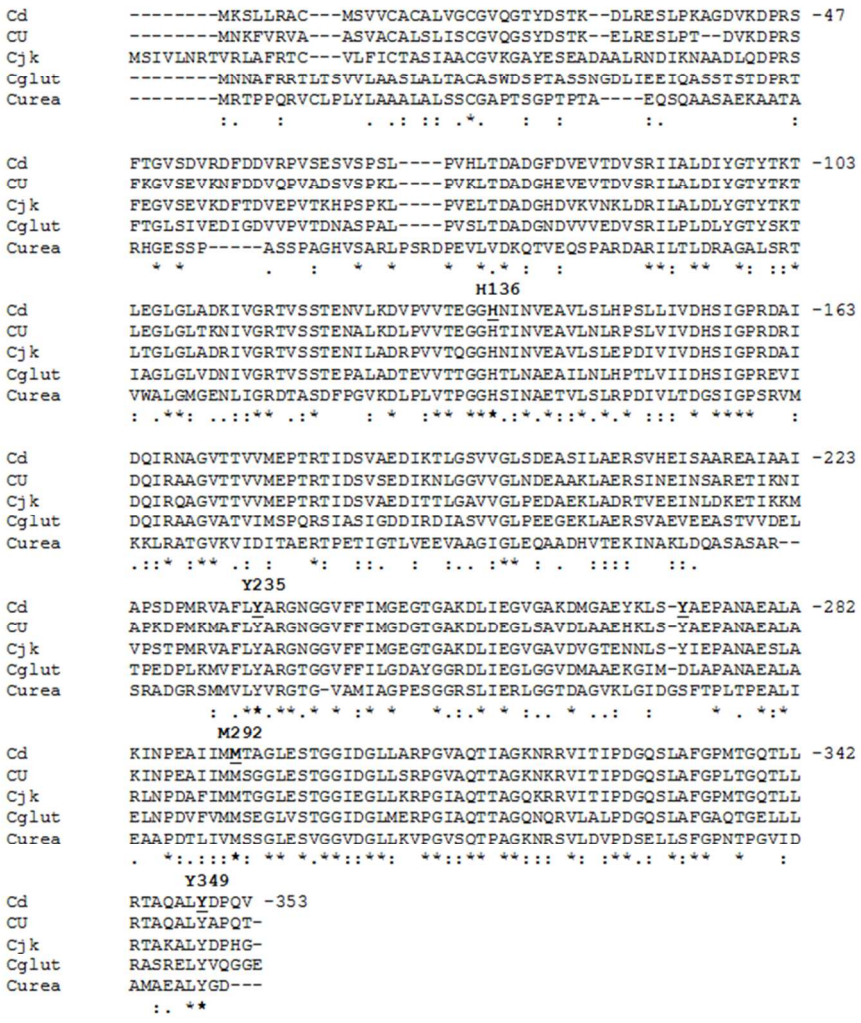

Figure S1. Alignment of the amino acid sequence of HmuT from various *Corynebacterium* species. Species are designated as follows: Cd: *C. diphtheriae* 1737/NCTC13129; CU: *C. ulcerans* 712; Cjk: *C. jeikeium* k411-jk0316; Cglut: *C. glutamicum* ATCC 13032; Curea: *C. urealyticum* DSM 7109. Conserved residues that were subjected to site-directed mutagenesis are indicated above the sequence alignment; asterisks indicate sequence identity and colons and periods show sequence similarity.

Figure S2. Alignment of the amino acid sequence of *Cd*HmuT with four HBPs with known crystal structures. Square boxes indicate the known axial ligands. Orange: *P. aeruginosa* PhuT (*1*) and *S. dysenteriae* ShuT (*1*). Green: *S. aureus* IsdE (*2*). Blue: *Y. pestis* HmuT (*3*). Red: *C. diphtheriae* HmuT. For *Cd*HmuT, M292 is also shown.

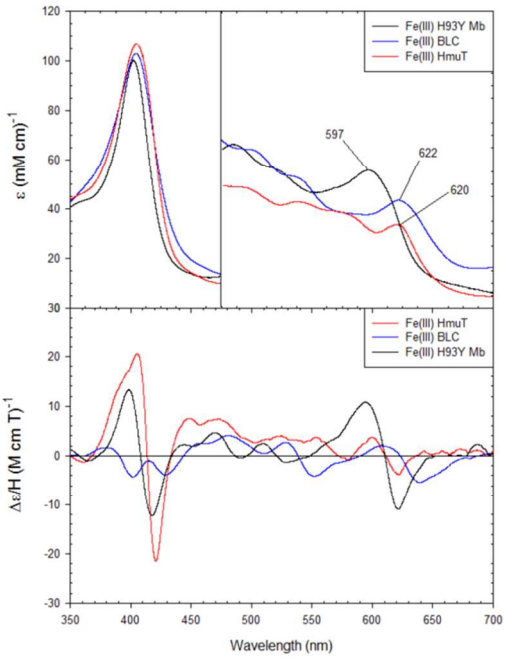

Figure S3. Comparison of the UV-visible absorption and MCD spectra for Fe(III) WT *Cd*HmuT at pH 6.5 with Fe(III) bovine liver catalase (BLC) and H93Y myoglobin. The samples were taken in 50 mM phosphate buffer. Spectra were slightly dependent on buffer conditions. The spectra of BLC and H93Y myoglobin were replotted from (*4-6*) and (*7*), respectively.

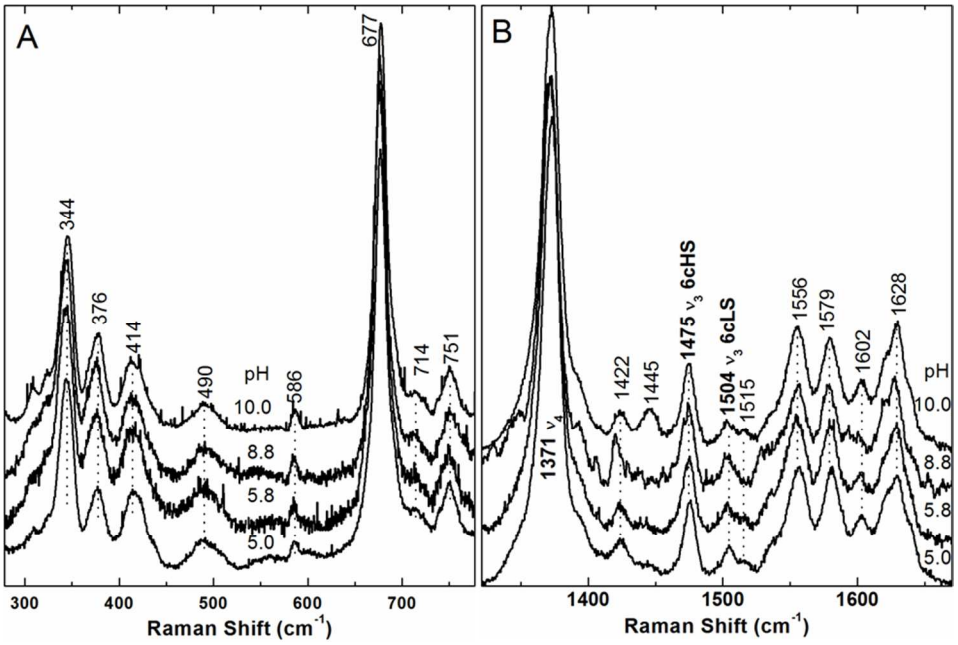

Figure S4. The rR spectrum of ferric WT *Cd*HmuT as a function of pH. A) Low frequency window. B) High frequency window. Protein concentration was 40 μM; excitation frequency of 413.1 nm was used with 9.4 mW laser power at the sample. The pH values are as indicated with the buffers described in the experimental section.

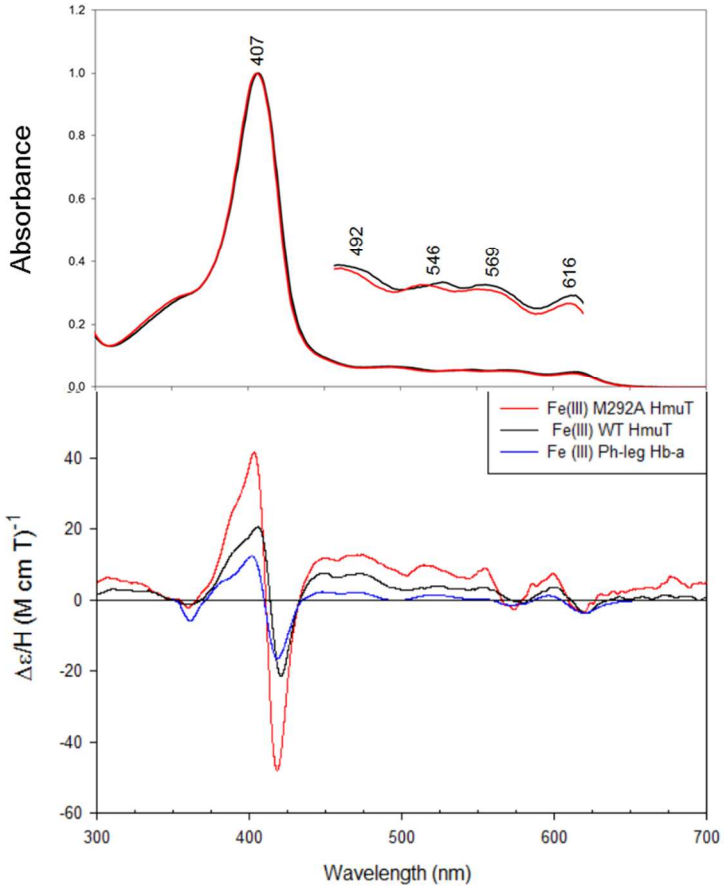

Figure S5. Top panel: UV-visible spectrum of WT *Cd*HmuT (black) and M292A *Cd*HmuT (red). The samples were taken in 50 mM Tris-Cl, pH 7.0. Bottom panel: Comparison of the MCD spectra for Fe(III) M292A *Cd*HmuT at pH 6.5 with Fe(III) WT *Cd*HmuT and Fe(III) phenol-leg Hb *a*. The samples were taken in 50 mM phosphate buffer. The spectrum of phenol-leg Hb *a* was replotted from (*8*).

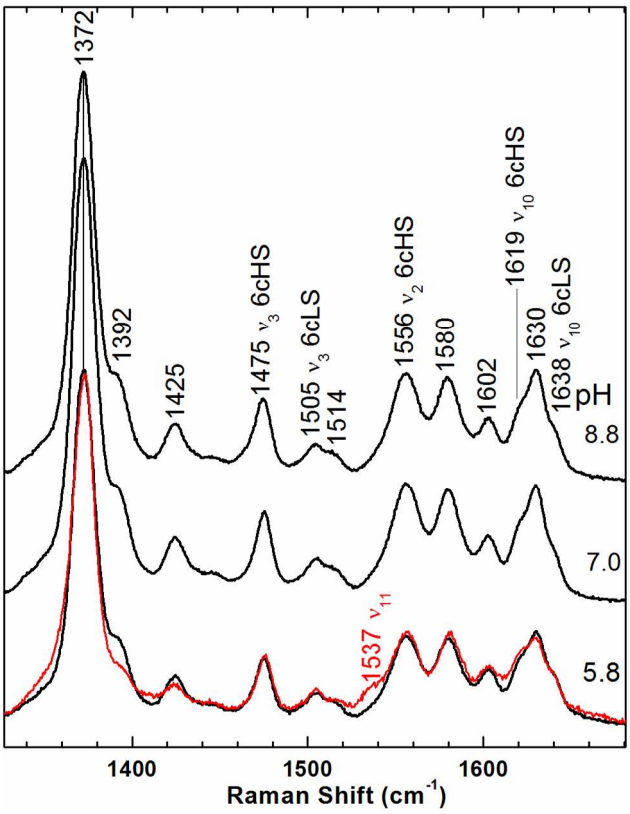

Figure S6. The rR spectrum of ferric M292A as a function of pH. Protein concentration was 36 μM; 406.7-nm excitation with 11 mW at the sample was used. The spectrum of ferric WT HmuT at pH 5.0 (red) is overlaid on the M292A pH 5.0 spectrum for comparison purposes. Coordination state and spin state markers ν_3, ν_2 and ν_{10} appear at the same frequencies in both spectra. The only noticeable difference between the WT and M292A spectra is the 1537 cm^{-1} shoulder, which is assigned to ν_{11} (the B_{1g}, C_β-C_β stretching mode) in the WT spectrum, and which is absent in the M292A spectrum.

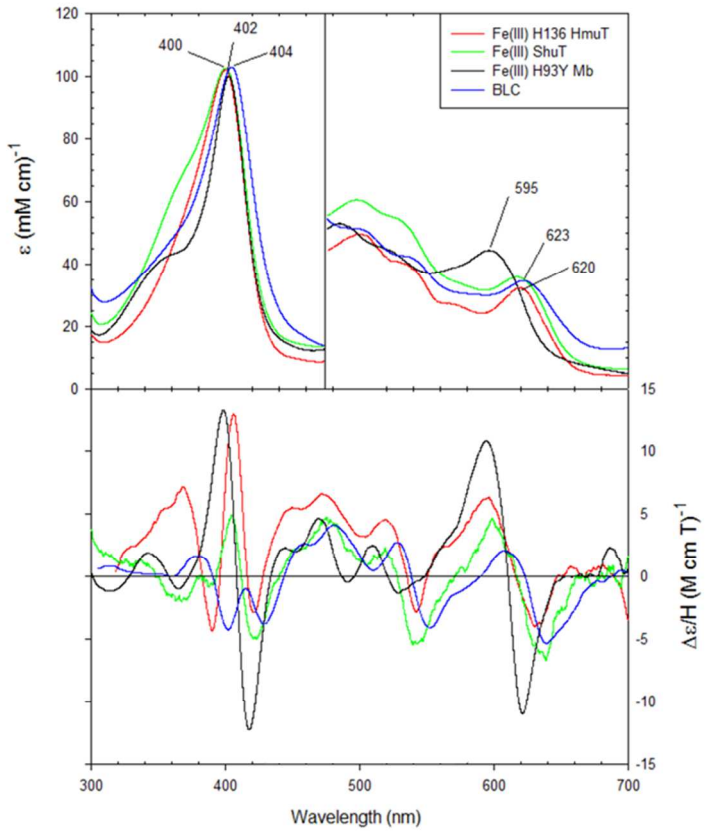

Figure S7. The UV-visible and MCD comparison spectra for Fe(III) H136A *Cd*HmuT at pH 6.5. Bottom panel: Comparison of the MCD spectra for Fe(III) H136A *Cd*HmuT with Fe(III) WT *Cd*HmuT, Fe(III) ShuT, Fe(III) H93Y Mb, and Fe(III) BLC. All samples in the work were taken in 50 mM phosphate buffer. Spectra of H93Y, ShuT, and BLC were replotted from (*7*),(*9*), and (*4-6*), respectively.

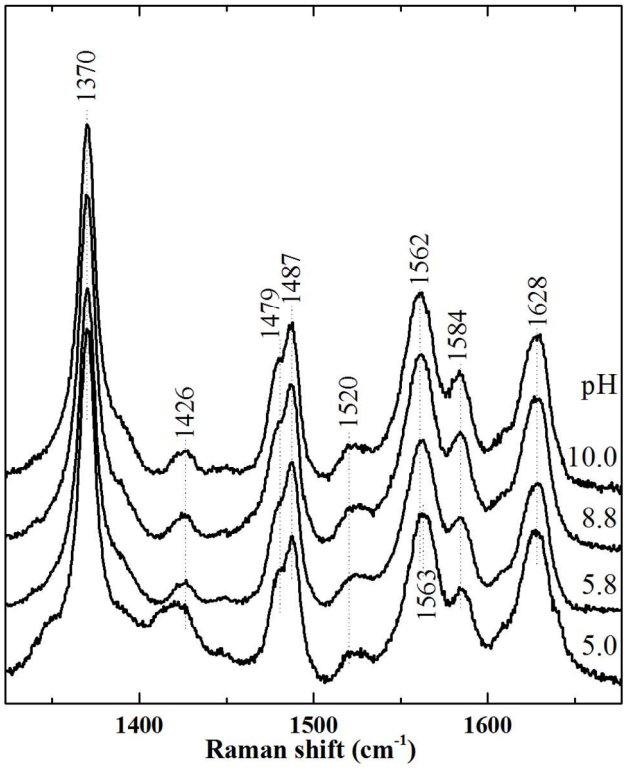

Figure S8. The rR spectrum of ferric H136A as a function of pH. Protein concentration was 25 μM; 406.7-nm excitation with 11 mW at the sample was used.

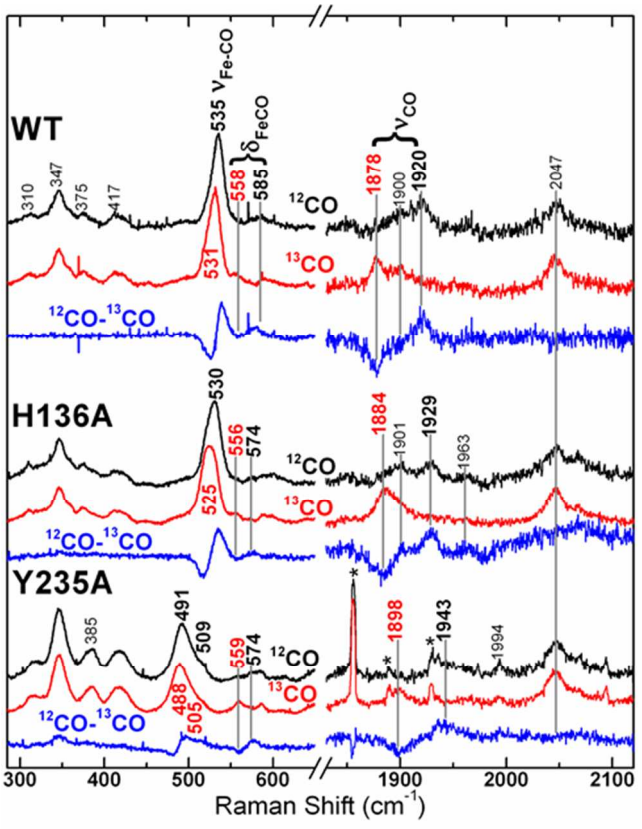

Figure S9. Resonance Raman spectra of the ferrous carbonyls of WT *Cd*HmuT, H136A, and Y235A recorded using 413.1-nm excitation. Natural abundance HmuT–CO (black), HmuT–^{13}CO (red) and difference (blue) spectra are shown for each protein. Spectra of WT and H136A were recorded at pH 8.8 and that of Y235A at pH 8.2. The asterisks in the carbonyl stretching region of the Y235A spectrum mark plasma emission lines from the Kr^+ laser.

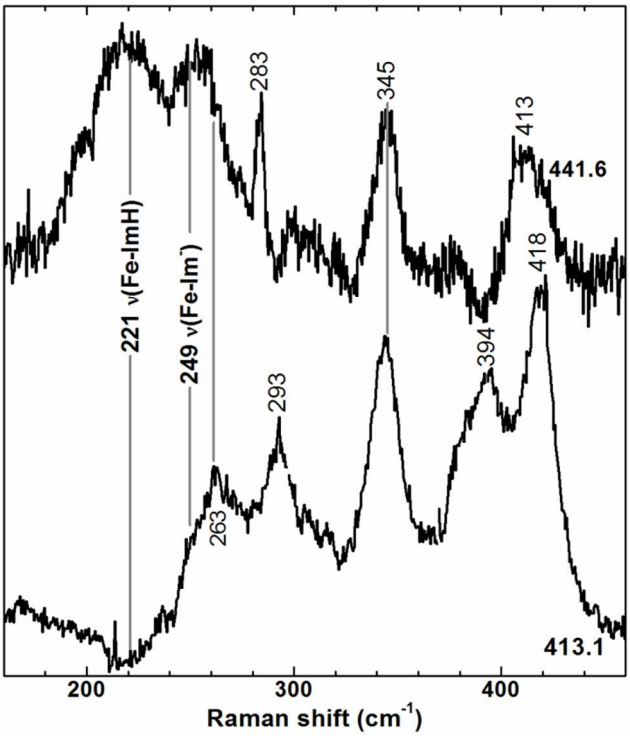

Figure S10. Comparison of the low frequency RR window of ferrous Y235A spectra obtained with 413.1-nm and 441.6-nm excitation. Laser powers at the sample were 4.0 mW and 4.6 mW, respectively. The solutions were 38 μM in protein and 100 mM in Tris-Cl, pH 8.8.

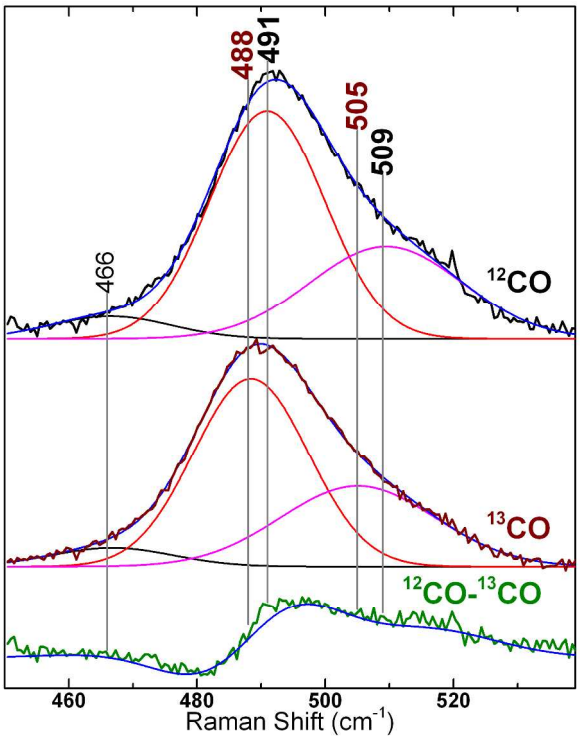

Figure S11. The Fe–C stretching region of the Y235A-CO rR spectrum. The experimental data for the natural abundance CO (black) and ^{13}CO (burgundy) complexes are shown with the peak fitting analysis of the 509/505 (magenta) and 491/488 cm^{-1} bands (red). Band widths are 24 and 18 cm^{-1}, respectively. The 466 cm^{-1} band is not ^{13}C sensitive. The simulated spectra are shown in blue; they are the sums of the fit peaks. The difference spectrum, obtained by subtraction of ^{13}CO spectrum from the natural abundance CO spectrum, is shown in green. The simulated ^{12}CO–^{13}CO difference spectrum (blue) is the difference between the simulated spectra for the ^{12}CO and ^{13}CO complexes.

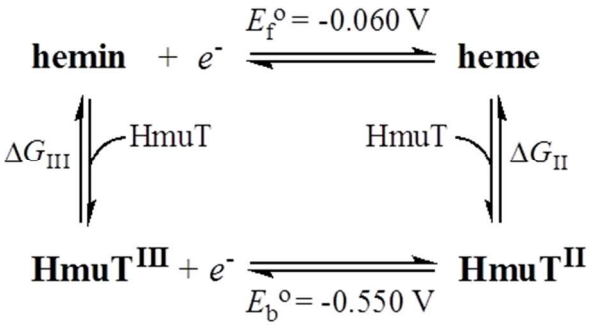

Figure S12. Thermodynamic cycle for heme binding and reduction.

Table S1. pK_a values of water *trans* to histidine in selected ferric heme proteins. The pK_a of ferrous microperoxidase 8 is reported as 10.9 (*10*).

Class	Protein	Fe(III)	Reference
CCOx	Cytochrome *c* oxidase	9.0	(*11*)
ClD	GR-1 chlorite dismutase	8.2	(*12*)
ClD	*Ideonella dechloratans* chlorite dismutase	8.5	(*13*)
ClD	*Dechloromonas aromatica* chlorite dismutase	8.7	(*14*)
FixL	*Rhizobium meliloti* FixL	9.3	(*15*)
FixL	*Bradyrhizobium japonicum* FixL	9.3	(*15*)
FixL	*Rhizobium meliloti* FixL	10	(*15*)
Hb	Leghemoglobin	8.3	(*16*)
Hb	Hemoglobin I (clam)	9.6	(*17*)
H-NOX	*Thermoanaerobacter tengcongensis* H-NOX	6.8	(*18*)
H-NOX	*Thermoanaerobacter tengcongensis* H-NOX I5L	7.9	(*18*)
H-NOX	*Thermoanaerobacter tengcongensis* H-NOX I5L/P115A	>10	(*18*)
H-NOX	*Thermoanaerobacter tengcongensis* H-NOX P115A	>10	(*18*)
HO	Heme oxygenase	7.6	(*19;20*)
HO	Mammalian HO-1	7.6	(*20*)
HO	Rat heme oxygenase-1	7.6	(*20*)
HO	*Pseudomonas aeruginosa* heme oxygenase	8.3	(*21*)
HO	Mammalian HO-2	8.5	(*22*)
HO	Bacterial heme oxygenase HmuO	9.0	(*23*)
HO	*Neisseriae meningitidis* heme oxygenase	9.3	(*24*)
HRP	Horseradish peroxidase	10.9	(*25*) (*26*)
IsdI	*Staphylococcus aureus* IsdI	7.1	(*27*)
Mb	Porcine myoglobin H64V/V68H/H93A/H97F	7.17	(*28*)
Mb	Aplysia myoglobin	7.6	(*25*)
Mb	Porcine myoglobin H64V/V68H/H93G/H97F	7.74	(*28*)
Mb	*Dolabella auricularia* myoglobin	7.8	(*29*)
Mb	Sperm whale myoglobin	8.95	(*25*)
MP	Microperoxidase 8	9.6	(*10;30*)

Table S2. Selected His/Tyr and Tyr heme-binding proteins with corresponding residues which are hydrogen-bonded to the axial tyrosine ligand. The examples are ordered by hydrogen bonding motif.

Protein	Axial Ligation	Residue Hydrogen Bonding to the Axial Tyrosine	Motif[a]	Soret Band	Q Bands				Reference
S. aureus IsdA	Y166	Y170	Yxxx**Y**	406	502	535		628	(*31*)
S. aureus IsdB-N2	Y440	Y444	Yxxx**Y**	406	504	540		630	(*32*)
S. aureus IsdC	Y132	Y136	Yxxx**Y**	403	502	533		627	(*33*)
S. aureus IsdH-N3	Y642	Y646	Yxxx**Y**	401	504	537		630	(*34*)
B. anthracis IsdX1	Y136	Y140	Yxxx**Y**	400	505	540		630	(*35*)
B. anthracis IsdX2-N5	Y108	Y112	Yxxx**Y**	404	500			630	(*36*)
P. aeruginosa HasA	H32/Y75	H83	Yxxxxxxx**H**	407	495	540	577	616	(*37*)
S. marcesans HasA	H32/Y75	H83	Yxxxxxxx**H**	406	494	537	568	618	(*38*)
Y. pestis HasA	Y75	H81	Yxxxxx**H**	403	498	535		620	(*39*)
Y. pestis HmuT	Y70/H167	R72[b]	Yx**R**	404					(*3*)
C. diphtheriae HmuT	H136/Y235	R273[c]	Yx**R**	407	492	546	569	616	This work
C. diphtheriae HmuT H136A	Y235	R273[c]	Yx**R**	400	504	546		620	This work
C. diphtheriae HmuT Y235A	H136	--	--	412		540	575		This work
P. aeruginosa PhuT	Y71	R73	Yx**R**	400	500	534		624	(*1*)

S. dysenteriae ShuT	Y67	K69[b]	Yx**K**	400	500	521		617	(*1*)
P. homomalla cAOS	Y353	R349	**R**xxxY	406	500	534		620	(*6*)
Bovine liver catalase	Y357	R353	**R**xxxY	404.5	500	535		622	(*6;40*)
M. avium ssp. *paratuberculosis* MAP	Y294	R290	**R**xxxY	406	503			621	(*6*)

[a] Residues in bold represent the amino acid hydrogen bonded to the axial ligand.

[b] Predicted that the residue could hydrogen bond the axial ligand, but is not directly observed in the crystal structure.

[c] Predicted that the residue could hydrogen bond the axial ligand via homology modeling and spectroscopic studies.

References

1. Ho, W. W., Li, H. Y., Eakanunkul, S., Tong, Y., Wilks, A., Guo, M. L., and Poulos, T. L. (2007) Holo-and apo-bound structures of bacterial periplasmic heme-binding proteins. *J. Biol. Chem. 282*, 35796-35802.

2. Grigg, J. C., Vermeiren, C. L., Heinrichs, D. E., and Murphy, M. E. (2007) Heme coordination by *Staphylococcus aureus* IsdE. *J. Biol. Chem. 282*, 28815-28822.

3. Mattle, D., Zeltina, A., Woo, J. S., Goetz, B. A., and Locher, K. P. (2010) Two stacked heme molecules in the binding pocket of the periplasmic heme-binding protein HmuT from *Yersinia pestis*. *J. Mol. Biol. 404*, 220-231.

4. Browett, W. R. and Stillman, M. J. (1979) Magnetic circular dichroism studies of bovine liver catalase. *Biochim. Biophys. Acta 577*, 291-306.

5. Abraham, B. D., Sono, M., Boutaud, O., Shriner, A., Dawson, J. H., Brash, A. R., and Gaffney, B. J. (2001) Characterization of the coral allene oxide synthase active site with UV-visible absorption, magnetic circular dichroism, and electron paramagnetic resonance spectroscopy: Evidence for tyrosinate ligation to the ferric enzyme heme iron. *Biochemistry 40*, 2251-2259.

6. Bandara, D. M. I., Sono, M., Bruce, G. S., Brash, A. R., and Dawson, J. H. (2011) Coordination modes of tyrosinate-ligated catalase-type heme enzymes: Magnetic circular dichroism studies of *Plexaura homomalla* allene oxide synthase, *Mycobacterium avium* ssp. paratuberculosis protein-2744c, and bovine liver catalase in their ferric and ferrous states. *J. Inorg. Biochem. 105*, 1786-1794.

7. Pond, A. E., Roach, M. P., Sono, M., Rux, A. H., Franzen, S., Hu, R., Thomas, M. R., Wilks, A., Dou, Y., Ikeda-Saito, M., Ortiz de Montellano, P. R., Woodruff, W. H., Boxer, S. G., and Dawson, J. H. (1999) Assignment of the heme axial ligand(s) for the ferric myoglobin (H93G) and heme oxygenase (H25A) cavity mutants as oxygen donors using magnetic circular dichroism. *Biochemistry 38*, 7601-7608.

8. Sievers, G., Gadsby, P. M., Peterson, J., and Thomson, A. J. (1983) Magnetic circular dichroism spectra of soybean leghaemoglobin *a* at room temperature and 4.2 K. *Biochim. Biophys. Acta 742*, 637-647.

9. Eakanunkul, S., Lukat-Rodgers, G. S., Sumithran, S., Ghosh, A., Rodgers, K. R., Dawson, J. H., and Wilks, A. (2005) Characterization of the periplasmic heme-binding protein ShuT from the heme uptake system of *Shigella dysenteriae*. *Biochemistry 44*, 13179-13191.

10. Vashi, P. R. and Marques, H. M. (2004) The coordination of imidazole and substituted pyridines by the hemeoctapeptide N-acetyl-ferromicroperoxidase-8 (Fe(II)NAcMP8). *J. Inorg. Biochem. 98*, 1471-1482.

11. Branden, M., Namslauer, A., Hansson, O., Aasa, R., and Brzezinski, P. (2003) Water-hydroxide exchange reactions at the catalytic site of heme-copper oxidases. *Biochemistry 42*, 13178-13184.

12. Hagedoorn, P. L., de Geus, D. C., and Hagen, W. R. (2002) Spectroscopic characterization and ligand-binding properties of chlorite dismutase from the chlorate respiring bacterial strain GR-1. *Eur. J. Biochem. 269*, 4905-4911.

13. Stenklo, K., Thorell, H. D., Bergius, H., Aasa, R., and Nilsson, T. (2001) Chlorite dismutase from *Ideonella dechloratans*. *J. Biol. Inorg. Chem. 6*, 601-607.

14. Streit, B. R., Blanc, B., Lukat-Rodgers, G. S., Rodgers, K. R., and Dubois, J. L. (2010) How active-site protonation state influences the reactivity and ligation of the heme in chlorite dismutase. *J. Am. Chem. Soc. 132*, 5711-5724.

15. Gilles-Gonzalez, M. A., Gonzalez, G., Perutz, M. F., Kiger, L., Marden, M. C., and Poyart, C. (1994) Heme-based sensors, exemplified by the kinase FixL, are a new class of heme protein with distinctive ligand binding and autoxidation. *Biochemistry 33*, 8067-8073.

16. Jones, D. K., Badii, R., Rosell, F. I., and Lloyd, E. (1998) Bacterial expression and spectroscopic characterization of soybean leghaemoglobin *a*. *Biochem. J. 330*, 983-988.

17. Kraus, D. W., Wittenberg, J. B., Lu, J. F., and Peisach, J. (1990) Hemoglobins of the *Lucina pectinata*/bacteria symbiosis. II. An electron paramagnetic resonance and optical spectral study of the ferric proteins. *J. Biol. Chem. 265*, 16054-16059.

18. Olea, C., Kuriyan, J., and Marletta, M. A. (2010) Modulating heme redox potential through protein-induced porphyrin distortion. *J. Am. Chem. Soc. 132*, 12794-12795.

19. Sun, J., Wilks, A., Demontellano, P. R. O., and Loehr, T. M. (1993) Resonance Raman and EPR spectroscopic studies on heme-heme oxygenase complexes. *Biochemistry 32*, 14151-14157.

20. Takahashi, S., Wang, J. L., Rousseau, D. L., Ishikawa, K., Yoshida, T., Host, J. R., and Ikedasaito, M. (1994) Heme-heme oxygenase complex structure of the catalytic site and its implication for oxygen activation. *J. Biol. Chem. 269*, 1010-1014.

21. Caignan, G. A., Deshmukh, R., Zeng, Y. H., Wilks, A., Bunce, R. A., and Rivera, M. (2003) The hydroxide complex of *Pseudomonas aeruginosa* heme oxygenase as a model of the low-spin iron(III) hydroperoxide intermediate in heme catabolism: C-13 NMR spectroscopic studies suggest the active participation of the heme in macrocycle hydroxylation. *J. Am. Chem. Soc. 125*, 11842-11852.

22. Ishikawa, K., Takeuchi, N., Takahashi, S., Matera, K. M., Sato, M., Shibahara, S., Rousseau, D. L., Ikedasaito, M., and Yoshida, T. (1995) Heme oxygenase-2 - Properties of the heme complex of the purified tryptic fragment of recombinant human heme oxygenase-2. *J. Biol. Chem. 270*, 6345-6350.

23. Chu, G. C., Tomita, T., Sonnichsen, F. D., Yoshida, T., and Ikeda-Saito, M. (1999) The heme complex of Hmu O, a bacterial heme degradation enzyme from *Corynebacterium diphtheriae* - Structure of the catalytic site. *J. Biol. Chem. 274*, 24490-24496.

24. Zeng, Y. H., Caignan, G. A., Bunce, R. A., Rodriguez, J. C., Wilks, A., and Rivera, M. (2005) Azide-inhibited bacterial heme oxygenases exhibit an S=3/2 (d(xz),d(yz))(3) (d(xy))(1)(d(z)(2))(1) spin state: Mechanistic implications for heme oxidation. *J. Am. Chem. Soc. 127*, 9794-9807.

25. Brunori, M., Amiconi, G., Antonini, E., Wyman, J., Zito, R., and Fanelli, R. (1968) Transition between acid and alkaline ferric heme proteins. *Biochim. Biophys. Acta 154*, 315-&.

26. Sitter, A. J., Shifflett, J. R., and Terner, J. (1988) Resonance Raman spectroscopic evidence for heme iron-hydroxide ligation in peroxidase alkaline forms. *J. Biol. Chem. 263*, 13032-13038.

27. Takayama, S. J., Ukpabi, G., Murphy, M. E. P., and Mauk, A. G. (2011) Electronic properties of the highly ruffled heme bound to the heme degrading enzyme IsdI. *Proc. Natl. Acad. Sci. USA 108*, 13071-13076.

28. Uno, T., Sakamoto, R., Tomisugi, Y., Ishikawa, Y., and Wilkinson, A. J. (2003) Inversion of axial coordination in myoglobin to create a "proximal" ligand binding pocket. *Biochemistry 42*, 10191-10199.

29. Yamamoto, Y., Chûjô, R., Inoue, Y., and Suzuki, T. (1992) Kinetic characterization of the acid-alkaline transition in *Dolabella auricularia* ferric myoglobin using ^{1}H-NMR saturation transfer experiments. *FEBS Lett. 310*, 71-74.

30. Munro, O. Q. and Marques, H. M. (1996) Heme-peptide models for hemoproteins. 2. N-acetylmicroperoxidase-8 - study of the pi-pi dimers formed at high ionic-strength using a modified version of molecular exciton theory. *Inorg. Chem. 35*, 3768-3779.

31. Grigg, J. C., Vermeiren, C. L., Heinrichs, D. E., and Murphy, M. E. P. (2007) Haem recognition by a *Staphylococcus aureus* NEAT domain. *Mol. Microbiol. 63*, 139-149.

32. Gaudin, C. F., Grigg, J. C., Arrieta, A. L., and Murphy, M. E. (2011) Unique heme-iron coordination by the hemoglobin receptor IsdB of *Staphylococcus aureus*. *Biochemistry 50*, 5443-5452.

33. Sharp, K. H., Schneider, S., Cockayne, A., and Paoli, M. (2007) Crystal structure of the heme-IsdC complex, the central conduit of the Isd iron/heme uptake system in *Staphylococcus aureus*. *J. Biol. Chem. 282*, 10625-10631.

34. Watanabe, M., Tanaka, Y., Suenaga, A., Kuroda, M., Yao, M., Watanabe, N., Arisaka, F., Ohta, T., Tanaka, I., and Tsumoto, K. (2008) Structural basis for multimeric heme complexation through a specific protein-heme interaction - The case of the third NEAT domain of IsdH from *Staphylococcus aureus*. *J. Biol. Chem. 283*, 28649-28659.

35. Ekworomadu, M. T., Poor, C. B., Owens, C. P., Balderas, M. A., Fabian, M., Olson, J. S., Murphy, F., Balkabasi, E., Honsa, E. S., He, C., Goulding, C. W., and Maresso, A. W. (2012) Differential function of Lip residues in the mechanism and biology of an anthrax hemophore. *PLoS Path. 8*.

36. Honsa, E. S., Owens, C. P., Goulding, C. W., and Maresso, A. W. (2013) The near-iron transporter (NEAT) domains of the anthrax hemophore IsdX2 require a critical glutamine to extract heme from methemoglobin. *J. Biol. Chem. 288*, 8479-8490.

37. Alontaga, A. Y., Rodriguez, J. C., Schonbrunn, E., Becker, A., Funke, T., Yukl, E. T., Hayashi, T., Stobaugh, J., Monne-Loccoz, P., and Rivera, M. (2009) Structural characterization of the hemophore HasAp from *Pseudomonas aeruginosa*: NMR spectroscopy reveals protein-protein interactions between holo-HasAp and hemoglobin. *Biochemistry 48*, 96-109.

38. Arnoux, P., Haser, R., Izadi, N., Lecroisey, A., Delepierre, M., Wandersman, C., and Czjzek, M. (1999) The crystal structure of HasA, a hemophore secreted by *Serratia marcescens*. *Nature Struct. Biol. 6*, 516-520.

39. Kumar, R., Lovell, S., Matsumura, H., Battaile, K. P., Moenne-Loccoz, P., and Rivera, M. (2013) The hemophore HasA from *Yersinia pestis* ($HasA_{yp}$) coordinates hemin with a single residue, Tyr75, and with minimal conformational change. *Biochemistry 52*, 2705-2707.

40. Fita, I. and Rossmann, M. G. (1985) The active center of catalase. *J. Mol. Biol. 185*, 21-37.